

DOI: 10.17725/rensit.2020.12.095

Polarimetry as a method for studying the structure of aqueous carbohydrate solutions: correlation with other methods

Anna V. Orlova, Leonid O. Kononov

Zelinsky Institute of Organic Chemistry of RAS, <http://zioc.ru/>
Moscow 119991, Russian Federation

E-mail: zozoka@gmail.com, leonid.kononov@gmail.com

Received February 12, 2020; peer reviewed February 18, 2020; accepted February 24, 2020

Abstract. The review provides data indicating that polarimetry is a sensitive tool for studying the structure of aqueous carbohydrate solutions. Using aqueous solutions of D-levoglucosan (1,6-anhydro-D-glucopyranose) as an example, it was demonstrated, using polarimetry, quantum chemical calculations, HPLC, static and dynamic light scattering, that polarimetry allows one to detect changes in the structure of solutions with changes in concentration and temperature, as well as the evolution of the structure of solutions over time. In particular, the phenomenon of the existence of “critical” concentrations and temperatures was discovered at which the specific rotation of the solutions undergo jump-like changes, apparently reflecting rearrangements in the structure of the solution. It is also possible that in the case of aqueous solutions, chiral carbohydrate molecules might act as “probes” that “sense” the slightest changes in their conformation or rearrangement of the environment (in the solvation shell) caused by changes in the structure of water, which at the macroscopic level manifests themselves as change in specific rotation.

Keywords: solution structure, supramers, polarimetry, light scattering, levoglucosan

UDC 547.455:543.454

Acknowledgement. This work was financially supported by the Russian Science Foundation (project No. 16-13-10244-P).

For citation: Anna V. Orlova, Leonid O. Kononov. Polarimetry as a method for studying the structure of aqueous carbohydrate solutions: correlation with other methods. *RENSIT*, 2020, 12(1):95-106; DOI: 10.17725/rensit.2020.12.095.

CONTENTS

1. INTRODUCTION (95)
 2. MATERIALS AND METHODS (96)
 - 2.1. MATERIALS (96)
 - 2.2. METHODS (96)
 - 2.2.1. Polarimetry (96)
 - 2.2.2. High Performance Liquid Chromatography (96)
 - 2.2.3. Dynamic light scattering (97)
 - 2.2.4. Static light scattering (97)
 3. RESULTS AND DISCUSSION (97)
 4. CONCLUSION (103)
- REFERENCES (103)

1. INTRODUCTION

It has been established [1-16] that the majority of macroscopically homogeneous aqueous and non-aqueous solutions of various *low molecular weight* substances used in everyday life and

ordinary laboratory practice are structured (inhomogeneous) at the nano and meso levels. The size of heterogeneities, supramers in our terminology [8], varies from ~ 1 nm to 10^2 – 10^3 nm. This new type of “weak” (judging by the magnitude of the interaction energy, which does not exceed $k_b T$ [17]), but the extremely effective and spontaneous structuring of liquids has not attracted the attention of researchers for a long time. Only recently has its importance been identified for an adequate description of reactions and other chemical processes [8, 9, 13, 14, 18-29].

For rational discussion of this complex situation in solution and the reactions involving solutes, we supposed that in many cases the real reactive species in solution are not isolated solute molecules but rather their supramolecular aggregates (which

we, for a reason, call supramers). The supramer approach is based on the assumption that the molecules of solutes can form stable homo- and hetero-supramers (which may also include solvent molecules [8]), the structure of which determines the observed reactivity, yield and selectivity of the reaction. More detailed discussion of these issues can be found in a recent review [8], devoted to an interconnection between chemical reactivity and the structure of the reaction solution.

For practical application of the supramer approach one must distinguish solutions of the same reagent, characterized by the presence of different supramers and consequently exhibiting different chemical properties [8]. For discrimination of solutions, differing in supramer composition (i.e., with different solution structure) we proposed to use polarimetry – measurement of the optical rotation of solutions in question. Indeed, specific optical rotation is not a feature of the molecular structure of the solute [30]. Even small conformational changes can lead to enormous changes in the specific rotation [31]. If these changes depend on the concentration, they are usually thought to be associated with aggregation of solute molecules [32]. Therefore, it can be expected that supramers consisting of molecules in a different conformation or differing in the way they are packed [33] or solvated [34], will also differ in the values of specific rotation.

2. MATERIALS AND METHODS

2.1. MATERIALS

Compounds **1** and **2** were prepared and purified according to the described procedures [34, 35]. Ultrapure water with a resistivity of $>18 \text{ M}\Omega \cdot \text{cm}$ (OMNI-A water purification system (PRC), using distilled water as the source) was used for preparation of aqueous solutions and chromatography. Solutions for physicochemical studies were prepared immediately before measurements by dissolving a weighed amount in a solvent in a volumetric flask (2 mL) and then filtering (4 times) the resulting solution through a membrane filter (0.45 μm , PTFE, diameter 13 mm, Chromafil (Macherey-Nagel, Germany); a separate filter was used for each sample).

2.2. METHODS

2.2.1. Polarimetry

Measurements of the optical rotation was performed on automatic digital polarimeters JASCO DIP-360 (Japan) (Fig. 9b), PU-7 (Russia) (Fig. 2, 6), or JASCO P-2000 (Japan) (Fig. 7, 8) in a glass jacketed polarimeter cell (length 10 cm). The temperature was maintained within $\pm 0.2^\circ\text{C}$ (DIP-360 and PU-7) or $\pm 0.1^\circ\text{C}$ (P-2000) by the circulation thermostats MLW U-1 (GDR) (when using DIP-360 and PU-7) or Huber CC-K6 (Exclusive) (Germany) (when using P-2000). Optical rotation value for each sample was measured only after stabilization of the temperature and the instrument readings (~ 30 min); after this, the instrument readings remained unchanged for several hours. Processing results in the case of use polarimeters JASCO DIP-360 and PU-7 involved finding an average of 10 measurements; standard deviations were calculated using Student's distribution (95%) and were (for both observed and specific rotation) less than 1% (unless otherwise indicated in the graphs).

In the case of measuring optical rotation on a JASCO P-2000 polarimeter, for each temperature, three independent freshly prepared solutions were used (unless otherwise indicated). For each solution, the optical rotation was measured for 30 min (1800 points with an integration time of 1 s). The data obtained were averaged, the error was calculated as the standard deviation from the mean. Additionally, average values and standard deviations were calculated for samples including specific rotation values for two temperature ranges: $12\text{--}25^\circ\text{C}$ and $32\text{--}55^\circ\text{C}$. The results are shown in Fig. 7, 8.

2.2.2. High Performance Liquid Chromatography (HPLC)

High-performance liquid chromatography of D-levoglucosan (**1**) samples was carried out at $85.0 \pm 0.1^\circ\text{C}$ on a Rezex RCM-Monosaccharide Ca^{+2} (8%) column (300 \times 7.8 mm) (Phenomenex, USA) with ultrapure water as the eluent at $0.6 \text{ mL} \cdot \text{min}^{-1}$ flow rate. A Waters 1122 column thermostat (USA) equipped with an aluminum heat exchanger with eight-millimeter sockets was used to maintain the column temperature.

The samples of solutions of D-levoglucosan were injected onto the column using a Reodyne 7125 injector (USA) with a 20 μL sample loop. A Gilson Model 155 UV detector (France), a Knauer 2300 differential refractometer (Germany), or an Alltech 2000ES ELSD detector (USA) were used for detection. The elution profile expressed as the ratio of absorbances at 195 nm and 205 nm (A^{195}/A^{205} detection) was obtained using a standard option (Real Time Ratio channel) built into the Gilson Model 155 UV detector.

2.2.3. Dynamic light scattering (DLS)

The intensities of scattered light were measured using an ALV 5000/6010 correlator goniometer system (Langen, Germany) at a scattering angle of 150° using Pyrex cells 1 cm in diameter and a He—Ne laser (633 nm, 23 mW) as the light source. The temperature of the scattering cell was maintained with an accuracy of $\pm 0.2^\circ\text{C}$. To obtain the correlation functions of scattered light intensity fluctuations, $[g^2(\tau)]$, the experimental data were averaged over 20 independent measurements (total time of the experiment was 20 min) and then processed using the CONTIN algorithm to calculate the contributions to the scattered intensity (so-called intensity-weighted size distribution) from particles of each observed size and to determine the correlation radii (hydrodynamic radii, R_h) of the light-scattering particles (and the corresponding correlation times) that were calculated at the maxima of the intensity-weighted size distribution [36].

2.2.4. Static light scattering (SLS)

Measurements of the intensity of the scattered light was performed as described in Section 2.2.3 for DLS. The intensity of the scattered light was averaged over a 20-minute interval for each solution. The SLS data were used to construct a modified Debye plot of C/R_θ as a function

of sample concentration (C), in which the sign of the slope (that is proportional to the second virial coefficient A_2) indicates the thermodynamic quality of solvent [36]. R_θ is the coefficient of scattering intensity at a scattering angle θ (an absolute scattering intensity defined as the ratio of scattered light intensity at a scattering angle θ to incident light intensity; Rayleigh ratio).

3. RESULTS AND DISCUSSION

A detailed study of the possibility of using polarimetry to study the structure of solutions was carried out on aqueous solutions of D-levoglucosan (**1**, 1,6-anhydro-D-glucopyranose, see Fig. 1a). Molecules **1** have a rigid structure in which conformational changes are possible only due to a change in the position (rotation) of hydroxy groups, which greatly simplifies quantum chemical calculations and interpretation of the results.

Using quantum chemical calculations (TD-DFT/GIAO), it was shown [34] that significant changes in the optical rotation value can be associated with slight distortions of the conformation of the levoglucosan molecule (calculations revealed 15 unique conformers) upon solvation caused by changes in the microenvironment of the levoglucosan molecule (Fig. 1b). The solvent was taken into account both within the polarizable continuum model (PCM) and by adding explicit water molecules (MS + PCM) [37]. For example, the calculated (PCM (H_2O)/B3LYP/6-311++G(2d,2p)//B3LYP/6-31+G(d,p)) specific optical rotation value for the GGG conformer is $-5.46 \text{ deg}\cdot\text{dm}^{-1}\cdot\text{cm}^3\cdot\text{g}^{-1}$. The addition of one water molecule significantly changes the calculated specific rotation ($-42.98 \text{ deg}\cdot\text{dm}^{-1}\cdot\text{cm}^3\cdot\text{g}^{-1}$). When a second water molecule is added, the specific rotation practically does not change (-42.97

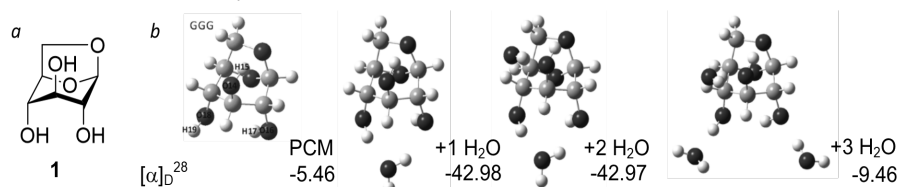


Fig. 1. The structure of D-levoglucosan (a); a change in the calculated (PCM/B3LYP/6-311++G(2d,2p)//B3LYP/6-31+G(d,p)) specific optical rotation of one of the conformers (GGG) of levoglucosan upon successive addition of water molecules (b) [34].

$\text{deg}\cdot\text{dm}^{-1}\cdot\text{cm}^3\cdot\text{g}^{-1}$). Conversely, the addition of a third water molecule again changes the calculated specific rotation to $-9.46 \text{ deg}\cdot\text{dm}^{-1}\cdot\text{cm}^3\cdot\text{g}^{-1}$. Thus, significant changes in the optical rotation can be caused by changes in the solvation shell, i.e. redistribution of solvent molecules around solute molecules (microsolvation, MS). These data indicate the promise of using polarimetry to study the microenvironment [37, 38] of solute molecules in solutions with different structures, as well as for detecting rearrangements of supramers in solutions.

An experimental study of the structure of aqueous solutions of levoglucosan using polarimetry began with freshly prepared solutions. The concentration dependence of the specific rotation of aqueous solutions of levoglucosan is nonlinear with discontinuities at concentrations of 0.1, 0.3, 0.5, and 1 $\text{mol}\cdot\text{L}^{-1}$ (Fig. 2). We called these concentrations “critical” and suggested that

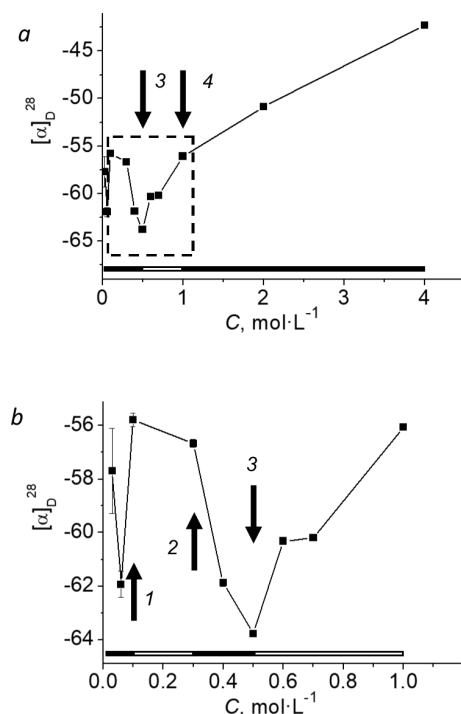


Fig. 2. Concentration dependences of specific rotation ($[\alpha]_D / \text{deg}\cdot\text{dm}^{-1}\cdot\text{cm}^3\cdot\text{g}^{-1}$) for freshly prepared aqueous solutions of levoglucosan [34]: the full range of studied concentrations (a); diluted solutions region (b). Here and in the following figures, the horizontal black and white bands near the concentration axis show the ranges of solution concentrations between the “critical” concentrations (0.1 (1), 0.3 (2), 0.5 (3) and 1.0 $\text{mol}\cdot\text{L}^{-1}$ (4); marked by vertical arrows), where supramers with different structures can exist.

they separate the areas of existence of different supramers.

A relationship between the detected “critical” concentrations and changes in the structure of the solution was established when studying the same solutions using static and dynamic light scattering (SLS and DLS) [34]. The dependence of the scattered light intensity (SLS data) on the concentration, shown as Debye plot (Fig. 3a), exhibits two extrema (0.5 and 1 $\text{mol}\cdot\text{L}^{-1}$), at which the slope changes. The slope is proportional to the second virial coefficient A_2 , the sign of which indicates the thermodynamic “quality” of solvent is [36]. Thus, in this case, at concentrations of solutions lower than 0.05 and greater than 1 $\text{mol}\cdot\text{L}^{-1}$, the solvent is good ($A_2 > 0$), while at the intermediate concentrations the solvent poor ($A_2 < 0$).

The DLS data indicate the presence of light scattering particles of various sizes in the solutions (Fig. 3b). At solution concentrations above 1 $\text{mol}\cdot\text{L}^{-1}$, only nano-sized supramers exist; in the concentration range 0.5–1 $\text{mol}\cdot\text{L}^{-1}$,

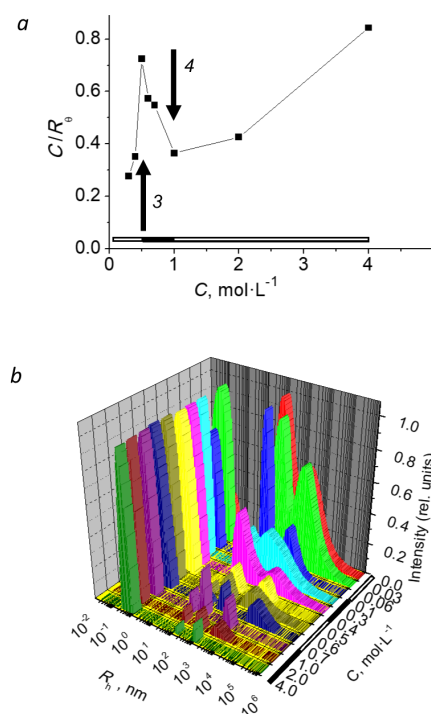


Fig. 3. Light scattering by freshly prepared aqueous solutions of levoglucosan depending on the concentration [34]. The concentration dependence of the intensity of the scattered light shown as the Debye plot (a). The intensity distribution of the size of the correlation radii (R_c) of light scattering particles (b).

larger supramers are added to them; in the range 0.3–0.5 mol·L⁻¹, the number of large supramers increases, and in ranges 0.1–0.3 mol·L⁻¹ large supramers predominate. Thus, DLS revealed the same “critical” concentrations (0.1, 0.3, 0.5, and 1 mol·L⁻¹) that were detected using polarimetry and SLS.

The same “critical” concentrations were detected using ligand exchange HPLC on a monosaccharide analysis column (Rezex RCM-Monosaccharide Ca²⁺) when eluting with water [39]. The elution profile, expressed as the absorption ratio at 195 nm and 205 nm (hereinafter referred to as A¹⁹⁵/A²⁰⁵ detection), varied greatly depending on the concentration of the sample of levoglucosan loaded on the column (Fig. 4).

A detailed analysis of the shape of peaks on chromatograms (A¹⁹⁵/A²⁰⁵ detection) showed that one symmetric peak of levoglucosan is observed for the solutions with a concentration not higher than 0.1 mol·L⁻¹ (*t*_R = 22.04–22.06 min; see chromatograms 1–3 in Fig. 4). At concentrations 0.3 and 0.4 mol·L⁻¹, the top of the peak flattens (chromatograms 4 and 5 in Fig. 4), and starting from the concentration of 0.5 mol·L⁻¹, the peak splits into two components (*t*_R = 21.71–21.76 and 22.29–22.43 min; chromatograms 6–8 in Fig. 4). Starting from the concentration of 1.0 mol·L⁻¹, the “valley” between the two maxima becomes deeper and the retention times of the peak components noticeably change (*t*_R = 21.42–21.57 and 22.67–22.79 min; chromatograms 9–11 in Fig. 4). In other

words, a gradual increase in the concentration of levoglucosan in the injected solution leads to abrupt changes in the shape of the levoglucosan peak (A¹⁹⁵/A²⁰⁵ detection). These abrupt changes in the shape of the peak occur at the concentrations of 0.1, 0.5, and 1.0 mol·L⁻¹, which can reasonably be called “critical”. These “critical” concentrations are also clearly visible on the concentration dependence of the retention time of the peak of levoglucosan and its components (A¹⁹⁵/A²⁰⁵ detection) (see Fig. 5). It is important to note that these concentrations entirely correspond to the “critical” concentrations detected by us earlier [34] by polarimetry and light scattering, which suggests that the origins of these phenomena could have similar nature associated with the concerted changes in the solution structure upon changes in concentration.

The absence of rectangular peaks on chromatograms (A¹⁹⁵/A²⁰⁵ detection) (Fig. 4) means that the peak of levoglucosan is not the peak of an “individual compound” and is in fact a composite peak [40]. This also means that the UV spectra of the eluate differ depending on the concentration of the injected solution. One gets an impression that in a single chromatographic peak, which corresponds to the same solute (levoglucosan in our case), several “compounds” with different UV spectra are eluted from the column depending on the concentration of the injected sample. In our opinion, such “compounds” can only be the supramers of the

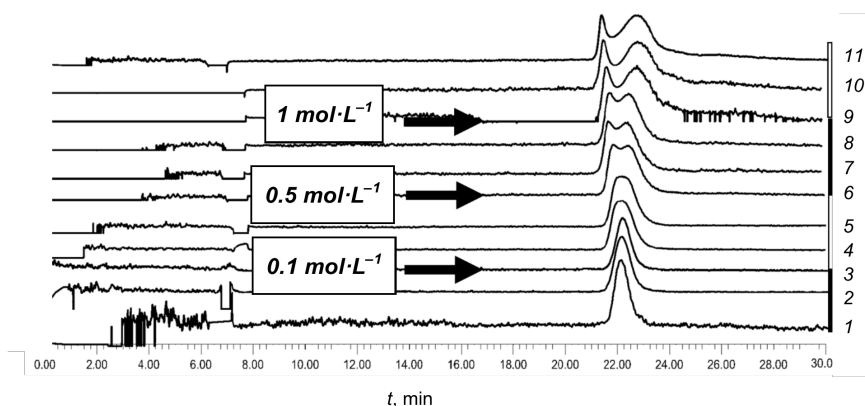


Fig. 4. HPLC elution profiles of samples of aqueous solutions of levoglucosan with concentrations of 0.03 (1), 0.06 (2), 0.1 (3), 0.3 (4), 0.4 (5), 0.5 (6), 0.6 (7), 0.7 (8), 1.0 (9), 2.0 (10) and 4.0 mol·L⁻¹ (11), expressed as the absorption ratio at 195 and 205 nm (A¹⁹⁵/A²⁰⁵) (see also Fig. 5) [39]. In the figure (on the right), vertical black and white bands indicate “conservative” concentration ranges between “critical” concentrations of 0.1, 0.5, and 1.0 mol·L⁻¹ (shown by arrows).

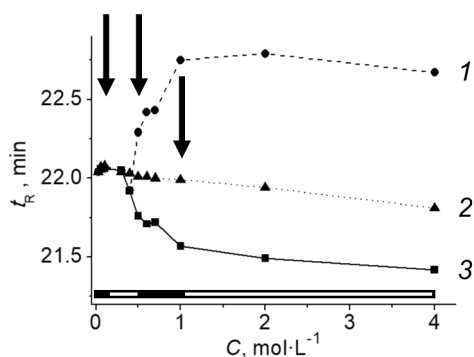


Fig. 5. Concentration dependence of the retention time (t_R /min) of the peak of levoglucosan (2) (A^{195} detection) and its components (A^{195}/A^{205} detection): the first (3) and second (1) peaks (see also Fig. 4) [39]. Horizontal black and white bands indicate “conservative” concentration ranges between “critical” concentrations of 0.1, 0.5, and 1.0 mol·L⁻¹ (shown by arrows).

solite. In this case, a serious argument in favor of this version is the above-described detection of the “critical” concentrations (0.1, 0.5, and 1.0 mol·L⁻¹) separating both the similar chromatographic profiles and the corresponding “conservative” concentration ranges, detected by SLS/DLS [34], in which similar supramers of levoglucosan are present in the solution. This observation may indicate an unexpectedly high stability of the levoglucosan supramers in solution, especially if the chromatographic conditions (85°C, 25 min) are taken into account.

A series of experiments was carried out to study the evolution of the structure of levoglucosan solutions over time [41]. Solutions with different concentrations were frozen and kept at -20°C, thawed to measure the optical rotation (Fig. 6).

Analysis of the concentration dependences (see Fig. 6) of the specific rotation values for freshly prepared solutions of levoglucosan and those kept at -20°C suggests that the form of the concentration plot does not change much for the solutions with concentrations equal to and higher than 1.0 mol·L⁻¹. However, considerable changes of specific rotation values were found for more dilute solutions: the specific rotation for solutions with a concentration of 0.1 mol·L⁻¹ (“critical” concentration 1) changes noticeably; however, the extremum is still at this point. Although the specific rotation value for solutions with a concentration of 0.5 mol·L⁻¹ (“critical” concentration 3) does

not remain constant, this concentration is featured by the local minima of the plot. It should also be noted that the specific rotation value is constant for solutions with concentrations of 0.3 and 1.0 mol·L⁻¹ (“critical” concentrations 2 and 4). Thus, many features of the concentration dependences of the specific rotation values observed for freshly prepared solutions (for example, some “critical” concentrations; see Fig. 2) are also preserved for samples kept frozen (see arrows in Fig. 6). This indicates that although levoglucosan solutions undergo evolution in time, these “critical” concentrations do not change [41].

This dynamics of aqueous solutions of levoglucosan manifests itself also with a change in temperature. To study the effect of temperature changes on the structure of the solution of levoglucosan [42], a concentration of 0.1 mol·L⁻¹ was chosen, which corresponds to the “critical”

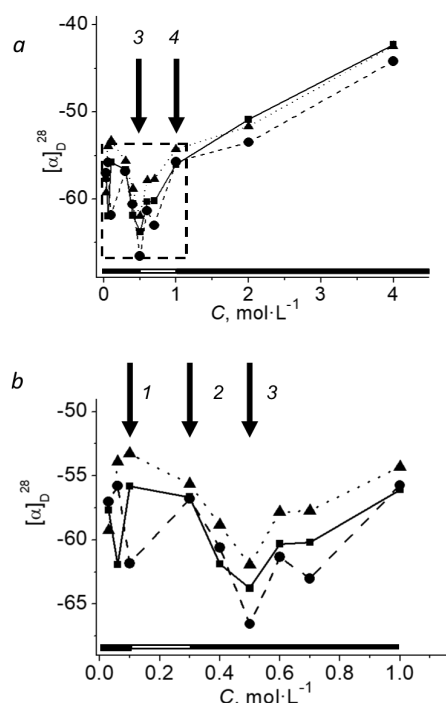


Fig. 6. The values of specific optical rotation ($[\alpha]_D^{28}/\text{deg}\cdot\text{dm}^{-1}\cdot\text{cm}^3\cdot\text{g}^{-1}$) for solutions of different concentrations of levoglucosan in water (mol·L⁻¹) 4[41]: 0.03–4.0 (a); 0.03–1.0 (b); freshly prepared solutions (solid line), the same solutions after storage for 7 (dashed line) and 14 days (dotted line) at a temperature of -20 °C. The critical concentrations of 0.1 (1), 0.3 (2), 0.5 (3) and 1.0 mol·L⁻¹ (4) are indicated by vertical arrows.

concentration 1 (Fig. 2) identified previously [34, 39, 41].

The study of the effect of temperature on the specific optical rotation of a solution of levoglucosan was started by heating one sample to different temperatures during one day. To this end, the prepared solution (solution # 1, Fig. 7a) was heated to a certain temperature, kept at this temperature for 10 min, and then optical rotation was measured for 30 min (1800 points with integration time of 1 s). The results were averaged; the error was calculated as the standard deviation from the mean. Then the same solution was heated to the next temperature, kept at the next temperature for 10 min, and optical rotation was measured for 30 min. The procedure was repeated. Comparison of the obtained data allowed us to detect a significant change in the specific optical rotation during the transition from a temperature of 28°C to a temperature of 44°C (Fig. 7a). For a more detailed study of the temperature dependence of specific optical rotation, a second solution was prepared (solution # 2, Fig. 7b),

which was heated during 3 days (intermittently). From the data obtained (Fig. 7b), the variability of the values of specific rotation measured on different days is clearly visible. The third solution (solution # 3, Fig. 7c) was not only heated, but also cooled. The data obtained indicate that the specific optical rotation varies greatly during measurements over several days. The main thing is that no regularities are visible in the change in the optical rotation of this solution with a change in temperature (Fig. 7c). This is especially evident when comparing the temperature dependences of the specific optical rotation values for each of these three solutions obtained during the first day after preparation (Fig. 7d). It is also seen that the difference between the specific optical rotation values for the same solution, measured on different days even at the same temperature, can be very large (cf. Fig. 7b,c). According to the results of these experiments, the following conclusion can be made: keeping the solutions of levoglucosan at different temperatures leads to irreproducible values of specific optical rotation. Apparently, the

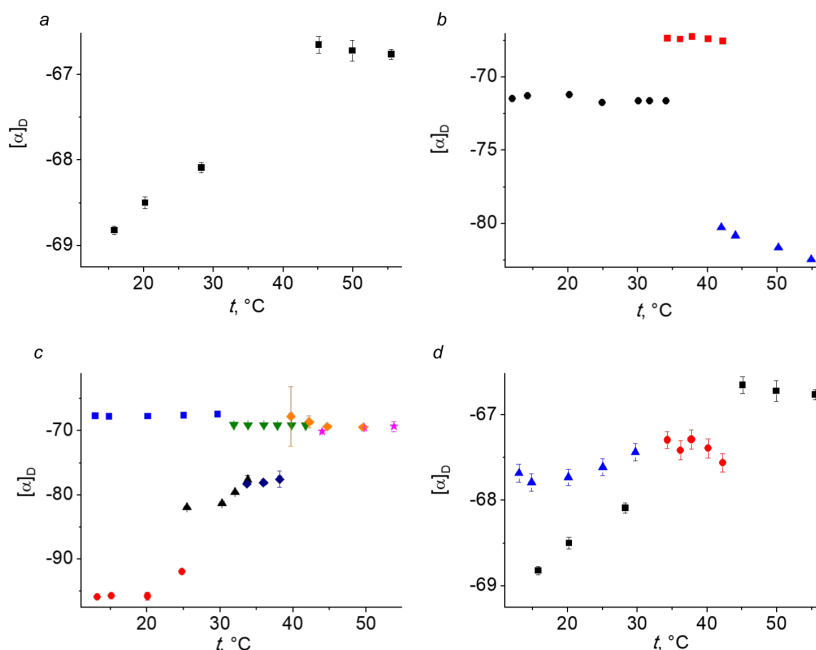


Fig. 7. Specific optical rotation ($[\alpha]_D / \text{deg} \cdot \text{dm}^{-1} \cdot \text{cm}^3 \cdot \text{g}^{-1}$) of aqueous solutions of levoglucosan with a concentration of $0.1 \text{ mol} \cdot \text{L}^{-1}$ at various temperatures [42]. Solution # 1, heated to different temperatures during one day (a). Solution # 2, heated to different temperatures during 3 days (b): heating on day 1 (red squares), day 2 (black circles) and day 3 (blue triangles). Solution # 3 at different temperatures during 8 days (c): heating on day 1 (blue squares), day 2 (green inverse triangles) and day 3 (purple stars); cooling on day 3 (orange hexagons), day 4 (dark blue diamonds), day 7 (black triangles), day 8 (red circles). Three solutions (see Fig. 7a,b,c) at different temperatures during the first day after preparation (d): solution # 1 (black squares), solution # 2 (red circles), solution # 3 (blue triangles).

measured values of specific optical rotation reflect the dynamics of the structure of these solutions.

The reproducibility problems were solved when the optical rotation of levoglucosan solutions at various temperatures was measured exclusively on freshly prepared solutions (in three repetitions for each concentration) [43].

In this case, on the graph of the specific optical rotation of aqueous solutions of levoglucosan with a concentration of $0.1 \text{ mol}\cdot\text{L}^{-1}$ on temperature (Fig. 8), two different temperature ranges can be distinguished in which specific rotation values differ (these differences are statistically significant ($t = 2.21, p < 0.05$)): from 12 to 25°C and from 32 to 55°C , separated by the “critical” temperature at 30°C . This temperature coincides with the “critical” temperature that we discovered earlier [44] (Fig. 9) when studying an aqueous solution of allyl lactoside (2) with a concentration of $0.2 \text{ mol}\cdot\text{L}^{-1}$, although in this case the effect of a step-like change in the properties of solutions at 30°C is much more noticeable.

Indeed, in the graph of the temperature dependence of the specific optical rotation of the allyl lactoside (2) solution, a small jump is

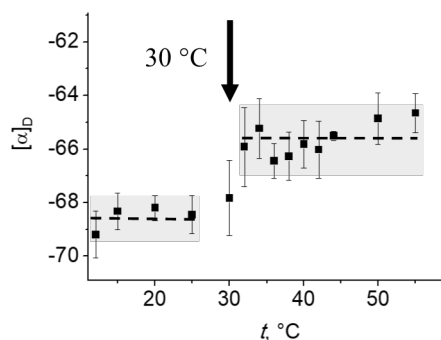


Fig. 8. Specific optical rotation ($[\alpha]_D/\text{deg}\cdot\text{dm}^{-1}\cdot\text{cm}^3\cdot\text{g}^{-1}$) of freshly prepared aqueous solutions of levoglucosan with a concentration of $0.1 \text{ mol}\cdot\text{L}^{-1}$ at various temperatures [43]. Each point represents the average value of specific rotation for three various solutions at a given temperature. The gray shaded indicate the areas: from 12 to 25°C ($[\alpha]_D = -68.6 \pm 0.8 \text{ deg}\cdot\text{dm}^{-1}\cdot\text{cm}^3\cdot\text{g}^{-1}$) and from 32 to 55°C ($[\alpha]_D = -65.6 \pm 1.1 \text{ deg}\cdot\text{dm}^{-1}\cdot\text{cm}^3\cdot\text{g}^{-1}$) the vertical size of the shaded region corresponds to the error calculated as the standard deviation from the mean, dashed lines indicate the average values for each sample. The arrow indicates a “critical” temperature of 30°C ($[\alpha]_D = -67.8 \pm 1.4 \text{ deg}\cdot\text{dm}^{-1}\cdot\text{cm}^3\cdot\text{g}^{-1}$).

observed at a temperature of 30°C (Fig. 9b) [44]. An additional confirmation that this temperature is “critical” is a sharp increase in the observed

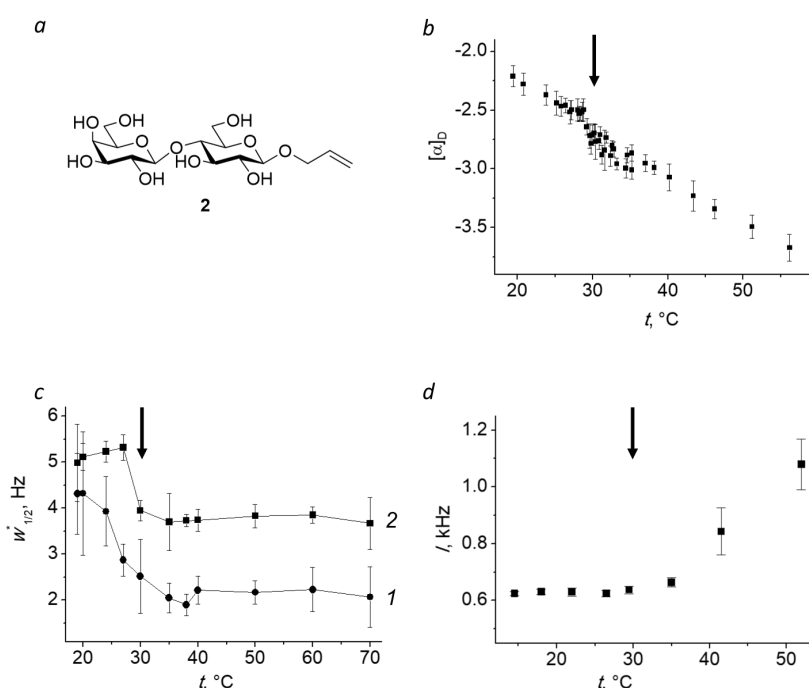


Fig. 9. The structure of allyl lactoside (2) (a). Temperature dependences for aqueous solutions of 2 with a concentration of $0.2 \text{ mol}\cdot\text{L}^{-1}$ [44]: specific rotation ($[\alpha]_D/\text{deg}\cdot\text{dm}^{-1}\cdot\text{cm}^3\cdot\text{g}^{-1}$) in H_2O (b); the width ($w_{1/2}/\text{Hz}$) of the signals ($\delta 4.50$ (1) and 5.25 ppm (2)) in the ^1H NMR spectrum of solution of 2 in D_2O (c); scattered light intensity (I/kHz) of solution of 2 in H_2O (d). The arrow indicates a “critical” temperature of 30°C .

resolution in ^1H NMR spectra at the same temperature (see temperature dependences of the observed signal width of one of the anomeric protons and one of the methylene protons of the double bond of the allyl group in Fig. 9c) and an increase in the intensity of light scattering (Fig. 9d) [44].

The coincidence of “critical” temperatures for aqueous solutions of two different derivatives of carbohydrates [43, 44], apparently, indicates a common cause of this phenomenon. It is possible that jump-like changes in the specific optical rotation of aqueous carbohydrate solutions with a change in temperature reflect significant changes in the structure of water [45, 46], and the molecules of chiral solutes (carbohydrates) act as “probes” that “sense” the slightest changes in their conformation or rearrangement of the microenvironment (in the solvation “shell”), which at the macroscopic level is manifested as a change in the magnitude of the specific rotation (see [19, 26] and references cited therein).

4. CONCLUSION

Thus, high sensitivity of polarimetry to changes in the structure of aqueous carbohydrate solutions was demonstrated, which follows from the correlation with the results obtained by other physicochemical methods. In particular, the phenomenon of the existence of “critical” concentrations and temperatures was discovered at which the specific rotation of the solutions undergo jump-like changes, apparently reflecting rearrangements of the solution structure. It is noteworthy that the values of the “critical” concentrations and temperatures found using polarimetry, at which jump-like changes in the specific rotation value occur, coincide the “critical” concentrations and temperatures detected using other methods (SLS/DLS, HPLC, NMR).

REFERENCES

1. Sedláč M. Large-scale supramolecular structure in solutions of low molar mass compounds and mixtures of liquids: 1. Light scattering characterization. *J. Phys. Chem. B*, 2006, 110(9):4329-4338, DOI: 10.1021/jp0569335.
2. Sedláč M. Large-scale supramolecular structure in solutions of low molar mass compounds and mixtures of liquids: II. Kinetics of the formation and long-time stability. *J. Phys. Chem. B*, 2006, 110(9):4339-4345, DOI: 10.1021/jp056934x.
3. Sedláč M. Large-scale supramolecular structure in solutions of low molar mass compounds and mixtures of liquids. III. Correlation with molecular properties and interactions. *J. Phys. Chem. B*, 2006, 110(28):13976-13984, DOI: 10.1021/jp061919t.
4. Sedláč M, Rak D. Large-Scale Inhomogeneities in Solutions of Low Molar Mass Compounds and Mixtures of Liquids: Supramolecular Structures or Nanobubbles? *J. Phys. Chem. B*, 2013, 117(8):2495-2504, DOI: 10.1021/jp4002093.
5. Sedláč M, Rak D. On the Origin of Mesoscale Structures in Aqueous Solutions of Tertiary Butyl Alcohol: The Mystery Resolved. *J. Phys. Chem. B*, 2014, 118(10):2726-2737, DOI: 10.1021/jp500953m.
6. Rak D, Ovadová M, Sedláč M. (Non)Existence of Bulk Nanobubbles: The Role of Ultrasonic Cavitation and Organic Solutes in Water. *J. Phys. Chem. Lett.*, 2019, 10(15):4215-4221, DOI: 10.1021/acs.jpcclett.9b01402.
7. Rak D, Sedláč M. On the Mesoscale Solubility in Liquid Solutions and Mixtures. *J. Phys. Chem. B*, 2019, 123(6):1365-1374, DOI: 10.1021/acs.jpcc.8b10638.
8. Kononov LO. Chemical Reactivity and Solution Structure: On the Way to a Paradigm Shift? *RSC Adv.*, 2015, 5(58):46718-46734, DOI: 10.1039/c4ra17257d.
9. Lagodzinskaya GV, Laptinskaya TV, Kazakov AI, Kurochkina LS, Manelis GB. Slow large-scale supramolecular structuring as a cause of kinetic anomalies in the liquid-phase oxidation with nitric acid. *Russ. Chem. Bull.*, 2016, 65(4):984-992, DOI: 10.1007/s11172-016-1401-4.
10. Zemb TN, Klossek M, Lopian T, Marcus J, Schoettl S, Horinek D, Prevost SF, Touraud D, Diat O, Marcelja S, Kunz W. How to explain microemulsions formed by solvent mixtures

- without conventional surfactants. *Proc. Natl. Acad. Sci. USA*, 2016, 113(16):4260-4265, DOI: 10.1073/pnas.1515708113.
11. Buchecker T, Krickl S, Winkler R, Grillo I, Bauduin P, Touraud D, Pfitzner A, Kunz W. The impact of the structuring of hydrotropes in water on the mesoscale solubilisation of a third hydrophobic component. *Phys. Chem. Chem. Phys.*, 2017, 19(3):1806-1816, DOI: 10.1039/c6cp06696h.
 12. Svard M, Renuka Devi K, Khamar D, Mealey D, Cheuk D, Zeglinski J, Rasmuson AC. Solute clustering in undersaturated solutions - systematic dependence on time, temperature and concentration. *Phys. Chem. Chem. Phys.*, 2018, 20(22):15550-15559, DOI: 10.1039/c8cp01509k.
 13. Lagodzinskaya GV, Laptinskaya TV, Kazakov AI. Supramolecular structuring of aqueous solutions of strong acids: manifestations in light scattering, NMR, and oxidation kinetics. Does liquid have a drop-like nature? 1. Nitric acid. *Russ. Chem. Bull.*, 2018, 67(10):1838-1850, DOI: 10.1007/s11172-018-2297-y.
 14. Lagodzinskaya GV, Laptinskaya TV, Kazakov AI. Supramolecular structuring of aqueous solutions of strong acids: manifestations in light scattering, NMR, and oxidation kinetics. Does liquid have a drop-like nature? 2. Perchloric acid. *Russ. Chem. Bull.*, 2018, 67(12):2212-2223, DOI: 10.1007/s11172-018-2358-2.
 15. Hahn M, Krickl S, Buchecker T, Jost G, Touraud D, Bauduin P, Pfitzner A, Klamt A, Kunz W. Ab initio prediction of structuring/mesoscale inhomogeneities in surfactant-free microemulsions and hydrogen-bonding-free microemulsions. *Phys. Chem. Chem. Phys.*, 2019, 21(15):8054-8066, DOI: 10.1039/c8cp07544a.
 16. Orlova AV, Laptinskaya TV, Kononov LO. The first example of detection of mesoscale particles in a solution of a low-molecular-mass compound in dichloromethane. *Russ. Chem. Bull.*, 2019, 68(7):1462-1464, DOI: 10.1007/s11172-019-2580-6.
 17. Zemb T, Kunz W. Weak aggregation: State of the art, expectations and open questions. *Curr. Opin. Colloid Interface Sci.*, 2016, 22:113-119, DOI: 10.1016/j.cocis.2016.04.002.
 18. Ahiadorme DA, Podvalnyy NM, Orlova AV, Chizhov AO, Kononov LO. Glycosylation of dibutyl phosphate anion with arabinofuranosyl bromide: unusual influence of concentration of the reagents on the ratio of anomeric glycosyl phosphates formed. *Russ. Chem. Bull.*, 2016, 65(11):2776-2778, DOI: 10.1007/s11172-016-1654-y.
 19. Kononov LO, Fedina KG, Orlova AV, Kondakov NN, Abronina PI, Podvalnyy NM, Chizhov AO. Bimodal Concentration-Dependent Reactivity Pattern of a Glycosyl Donor: Is the Solution Structure Involved? *Carbohydr. Res.*, 2017, 437:28-35, DOI: 10.1016/j.carres.2016.11.009.
 20. Orlova AV, Laptinskaya TV, Bovin NV, Kononov LO. Differences in reactivity of N-acetyl- and N,N-diacetylsialyl chlorides, caused by their different supramolecular organization in solutions. *Russ. Chem. Bull.*, 2017, 66(11):2173-2179, DOI: 10.1007/s11172-017-1999-x.
 21. Krickl S, Buchecker T, Meyer AU, Grillo I, Touraud D, Bauduin P, Konig B, Pfitzner A, Kunz W. A systematic study of the influence of mesoscale structuring on the kinetics of a chemical reaction. *Phys. Chem. Chem. Phys.*, 2017, 19(35):23773-23780, DOI: 10.1039/c7cp02134h.
 22. Jehannin M, Charton S, Corso B, Mohwald H, Riegler H, Zemb T. Structured solvent effects on precipitation. *Colloid Polym. Sci.*, 2017, 295(10):1817-1826, DOI: 10.1007/s00396-017-4153-2.
 23. Krickl S, Touraud D, Bauduin P, Zinn T, Kunz W. Enzyme activity of horseradish peroxidase in surfactant-free microemulsions. *J. Colloid Interface Sci.*, 2018, 516:466-475, DOI: 10.1016/j.jcis.2018.01.077.
 24. Krickl S, Jurko L, Wolos K, Touraud D, Kunz W. Surfactant-free microemulsions with cleavable constituents. *J. Mol. Liq.*, 2018, 271:112-117, DOI: 10.1016/j.molliq.2018.08.120.
 25. Stepanova EV, Podvalnyy NM, Abronina PI, Kononov LO. Length matters: one additional

- methylene group in a reactant is able to affect the reactivity pattern and significantly increase the product yield. *Synlett*, 2018, 29(15):2043-2045, DOI: 10.1055/s-0037-1610648.
26. Nagornaya MO, Orlova AV, Stepanova EV, Zinin AI, Laptinskaya TV, Kononov LO. The use of the novel glycosyl acceptor and supramer analysis in the synthesis of sialyl- α (2-3)-galactose building block. *Carbohydr. Res.*, 2018, 470:27-35, DOI: 10.1016/j.carres.2018.10.001.
 27. Myachin IV, Orlova AV, Kononov LO. Glycosylation in flow: effect of the flow rate and type of the mixer. *Russ. Chem. Bull.*, 2019, 68(11):2126-2129.
 28. Enami S, Ishizuka S, Colussi AJ. Chemical signatures of surface microheterogeneity on liquid mixtures. *J. Chem. Phys.*, 2019, 150(2):024702, DOI: 10.1063/1.5055684.
 29. Qiu J, Ishizuka S, Tonokura K, Colussi AJ, Enami S. Water Dramatically Accelerates the Decomposition of α -Hydroxyalkyl-Hydroperoxides in Aerosol Particles. *J. Phys. Chem. Lett.*, 2019, 10:5748-5755, DOI: 10.1021/acs.jpcclett.9b01953.
 30. Gawley RE. Do the terms "% ee" and "% de" make sense as expressions of stereoisomer composition or stereoselectivity? *J. Org. Chem.*, 2006, 71(6):2411-2416, DOI: 10.1021/jo052554w.
 31. Wilson SM, Wiberg KB, Murphy MJ, Vaccaro PH. The effects of conformation and solvation on optical rotation: Substituted epoxides. *Chirality*, 2008, 20(3-4):357-369, DOI: 10.1002/chir.20448.
 32. Goldsmith MR, Jayasuriya N, Beratan DN, Wipf P. Optical rotation of noncovalent aggregates. *J. Am. Chem. Soc.*, 2003, 125(51):15696-15697, DOI: 10.1021/ja0376893.
 33. Suarez M, Branda N, Lehn JM, Decian A, Fischer J. Supramolecular chirality: Chiral hydrogen-bonded supermolecules from achiral molecular components. *Helv. Chim. Acta*, 1998, 81(1):1-13, DOI: 10.1002/hlca.19980810102.
 34. Orlova AV, Andrade RR, da Silva CO, Zinin AI, Kononov LO. Polarimetry as a Tool for the Study of Solutions of Chiral Solutes. *ChemPhysChem*, 2014, 15(1):195-207, DOI: 10.1002/cphc.201300894.
 35. Kononov LO, Kornilov AV, Sherman AA, Zyryanov EV, Zatonsky GV, Shashkov AS, Nifant'ev NE. Synthesis of oligosaccharides related to HNK-1 antigen. 2. Synthesis of β -propyl 3'''-O-(3-O-sulfo- β -D-glucuronopyranosyl)-lacto-N-tetraoside. *Russ. J. Bioorg. Chem.*, 1998, 24(8):537-550 (in Eng.).
 36. Schärftl W. *Light Scattering from Polymer Solutions and Nanoparticle Dispersions*. 1 ed., Berlin, Heidelberg, Springer-Verlag, 2007, 191 p.
 37. Goulart PN, da Silva CO, Widmalm G. The importance of orientation of exocyclic groups in a naphthoxyloside: A specific rotation calculation study. *J. Phys. Org. Chem.*, 2017:e3708, DOI: 10.1002/poc.3708.
 38. Franca BA, da Silva CO. Specific rotation of monosaccharides: a global property bringing local information. *Phys. Chem. Chem. Phys.*, 2014, 16(26):13096-13102, DOI: 10.1039/c4cp01316f.
 39. Orlova AV, Tsvetkov DE, Kononov LO. Separation of levoglucosan supramers by high performance liquid chromatography. *Russ. Chem. Bull.*, 2017, 66(9):1712-1715, DOI: 10.1007/s11172-017-1945-y.
 40. Cheng H, Gadde RR. Absorbance Ratio Plots in High Performance Liquid Chromatography: Some Software Problems and Remedies. *J. Chromatogr. Sci.*, 1985, 23(5):227-230, DOI: 10.1093/chromsci/23.5.227.
 41. Orlova AV, Zinin AI, Kononov LO. Mutarotation in aqueous solutions of D-levoglucosan: a supramer approach. *Russ. Chem. Bull.*, 2014, 63(1):295-297, DOI: 10.1007/s11172-014-0429-6.
 42. Orlova AV, Kononov LO. Polyarimetriya kak metod izucheniya struktury rastvorov [Polarimetry as a method for studying the structure of solutions]. *Proceedings of the Second All-Russian conference "Physics of aqueous solutions"* (Moscow, 17-18 October 2019). Moscow, IGP RAS, 2019, p. 36-39, DOI: 10.24411/9999-012A-2019-10014 (in Russ.).
 43. Orlova AV, Kondakov NN, Zuev YF, Kononov LO. Temperature dependence of specific

- optical rotation of an aqueous levoglucosan solution. *Russ. Chem. Bull.*, 2018, 67(11):2155-2156, DOI: 10.1007/s11172-018-2346-6.
44. Kononov LO, Tsvetkov DE, Orlova AV. Conceivably the first example of a phase transition in aqueous solutions of oligosaccharide glycosides. Evidence from variable-temperature ^1H NMR and optical rotation measurements for a solution of allyl lactoside. *Russ. Chem. Bull.*, 2002, 51(7):1337-1338, DOI: 10.1023/a:1020981320040.
45. Bagchi B. *Water in biological and chemical processes: from structure and dynamics to function*. Cambridge, Cambridge University Press, 2013, 356 p.
46. Kaatze U. Water, the special liquid. *J. Mol. Liq.*, 2018, 259:304-318, DOI: 10.1016/j.molliq.2018.03.038.